Physics Letters B 811 (2020) 135889

Contents lists available at ScienceDirect

Physics Letters B

www.elsevier.com/locate/physletb

LHC dijet angular distributions as a probe for the dimension-six triple gluon vertex

Reza Goldouzian *, Michael D. Hildreth

Department of Physics, 225 Nieuwland Science Hall, University of Notre Dame, Notre Dame, IN 46556, USA

ARTICLE INFO

Article history:
Received 10 January 2020
Received in revised form 10 September 2020
Accepted 19 October 2020
Available online 29 October 2020
Editor: L. Rolandi

ABSTRACT

In the absence of a concrete discovery of new physics at the LHC, global analyses of the standard model effective field theory (SMEFT) are important to find and describe the impact of new physics beyond the energy reach of the LHC. Among the SMEFT operators that can be constrained via various measurements, the dimension six triple gluon operator involves neither the Higgs boson nor the top quark, yet its variation can have measurable effects on top and Higgs production. Without independent constraints on its impact, the sensitivity of measurements in the top and Higgs sectors to new physics is reduced. Previous analyses have used various techniques to constrain the influence of the triple gluon operator. We show that the dijet angular distribution is a powerful observable for probing the triple gluon operator because of the different helicity structure of the dimension-six interaction, namely the lack of a t-channel exchange term, as compared with expectations from QCD. Using this novel approach, we set the most stringent limit on the size of the triple gluon effective coupling by reinterpreting the results of a search for new phenomena in dijet events using 35.9 fb^{-1} of pp collision data collected at $\sqrt{s} = 13$ TeV performed by the CMS Collaboration.

1. Introduction

In the context of standard model effective field theory (SMEFT), a systematic global interpretation of experimental measurements is possible for finding hints of physics beyond the well-described Standard Model (SM) of particle physics. In this theoretical framework, the SM is merely a low-energy approximation to a more complete theory containing new physics at higher energy scales not accessible to today's colliders. In this formulation, the full Lagrangian includes new higher dimension operators (O_x) which are suppressed by powers of the new physics scale (Λ) [1,2],

$$\mathcal{L} = \mathcal{L}_{\text{SM}} + \mathcal{L}_{\text{eff}} = \mathcal{L}_{\text{SM}} + \sum_x \frac{C_x}{\Lambda^2} O_x + \dots , \tag{1}$$

where C_x stand for the corresponding dimensionless Wilson coefficients.

In the literature, dimension-6 operators that affect the measurements of top-quark and Higgs boson properties are studied in detail and are constrained using global fits to experimental data collected at the Large Hadron Collider (LHC) and elsewhere [3–5]. Among the operators affecting Higgs boson and top quark production processes, the triple-gluon operator involves neither the Higgs boson nor the top quark. However, this operator can contribute to the top quark production cross section and in processes involving additional jets, such as Higgs+jets, and thus its effects have large correlations with other operators involving new physics in the top or Higgs sectors [3,6]. Not constraining its contribution in global EFT fits can reduce the sensitivity to variations in the operators connected to the top quark or Higgs boson [6,7]. As discussed below, a recent analysis [8] has set strong constraints on the possible size of the contributions of the triple-gluon operator, and hence its potential influence on top and higgs physics, using the property that its effect should grow with jet energy and multiplicity. This paper presents a novel and complementary analysis with substantially higher sensitivity exploiting the helicity structure of the triple-gluon operator to produce new constraints on its effects.

The triple-gluon operator is the only CP-even dimension-6 genuinely gluonic operator consisting of three factors of the gluon field strength,

$$O_G = g_s f_{ABC} G_\mu^{A\nu} G_\nu^{B\rho} G_\rho^{C\mu} , \tag{2}$$

where $G^A_{\mu\nu} = \partial_\mu G^A_\nu - \partial_\nu G^A_\mu + g_s f^{ABC} G^B_\mu G^C_\nu$, f^{ABC} is the structure constant of SU(3), and g_s is the QCD coupling constant. In principle, the O_G operator affects three and four gluon vertices

* Corresponding author.
E-mail address: reza.goldouzian@cern.ch (R. Goldouzian).

https://doi.org/10.1016/j.physletb.2020.135889

and generates additional vertices with up to six gluons. So one might expect to observe the effects of this operator in inclusive jet production at high energy hadron colliders. However, it has been shown that the helicity structure of the amplitudes for the $gg \to gg$ and $gq \to gq$ processes which involve the gluon operator is orthogonal to that of pure quantum chromodynamics (QCD) at tree level [7,9,10]. Consequently, there is no interference between the QCD and O_G operator at leading order and the first non-zero contribution comes at $O(1/\Lambda^4)$. Alternative processes with non-zero interference such as three jet production [7,11] and heavy quark production [12,13] were suggested in order to constrain the effects of the O_G operator.

Recently in Ref. [8], the authors set a strong constraint on the C_G coefficient at 95% confidence level (CL), $C_G/\Lambda^2 < 0.04$ TeV^{-2}, using high-multiplicity jet measurements performed by the CMS Collaboration at 13 TeV. They have shown that, although the effects of the interference terms are negligible in multijet production, terms of order $O(1/\Lambda^4)$ are large enough to be observed in events with high S_T and a large number of jets. In this case, S_T is the scalar sum of jet transverse momentum plus any missing transverse momentum above 50 GeV. A detailed examination of this analysis, performed in Ref. [7] concluded that its results are valid and internally consistent. This examination includes evaluating the impact of the dimension-8 operators with the same expansion order in $1/\Lambda$ as the dimension-6-squared terms and the use of data in the high energy region (*i.e.*, at scales comparable to Λ) within the SMEFT framework. The same considerations and conclusions apply to the analysis strategy presented below.

In Ref. [7], it is shown that the increase of the O_G cross section over the SM cross section in the higher jet multiplicities is because of new partonic channels opening up with increasing number of outgoing partons. Another important difference between the parton production process via the O_G operator and the SM lies in the structure of the partonic cross section. In the O_G case, none of the $gg \to gg$, $gg \to qq$, $gq \to gq$, and $qq \to gg$ sub-process cross sections have a t-channel pole [10]. This is opposed to dijet production in the SM, where all sub-processes have a t-channel pole. This results in markedly different dijet angular distributions between the SM and O_G production processes.

At the LHC, the production of jets is largely used to validate the theory of QCD and to search for theories beyond the SM. Besides, the dijet angular distributions are an excellent tool to search for new physics [14–16]. Experimentally, the angular variable χ_{dijet} is defined as:

$$\chi_{dijet} = exp(|y_1 - y_2|) \tag{3}$$

where y_1 and y_2 are the rapidity of the two jets with the highest transverse momentum (p_T) in the laboratory frame. In the SM QCD, the angular distributions are approximately independent of χ_{dijet} since all scattering processes are dominated by the t-channel gluon exchange. Therefore, new physics contributions that have different production characteristics can be detected on top of the approximately uniform angular distributions expected in the SM. The dijet angular distributions are measured at the LHC by the ATLAS and CMS Collaborations at 7, 8 and 13 TeV and no significant deviation from the SM prediction is observed [17,18]. Within the SMEFT framework, the measured dijet angular distributions have traditionally been used to set constrains on the strength of four-fermion operators [19].

In this paper we propose the dijet angular distributions as a powerful observable for probing the triple gluon vertices at the LHC. Furthermore, we use the latest results of the dijet angular distributions measured by the CMS Collaboration at 13 TeV to set bounds on the C_G coupling [17].

2. Simulation

We use FeynRules [20] to implement the Lagrangian of the O_G operator and write it in Universal FeynRules Output (UFO) files [21]. The UFO files are then fed into the Madgraph@NLO Monte Carlo event generator for the event simulation and cross section calculation of the multijet processes [22]. Multijet events are generated at leading order (LO) with up to four outgoing partons using the LO NNPDF3.0 parton distribution function (PDF) set [23]. The factorization and renormalization scales are set to the average transverse momentum of the two leading jets in p_T. Generated events are passed to PYTHIA8 [24] for showering and hadronization with the underlying event tune CUETP8M1 [25]. The MLM matching scheme is used to remove any double-counting between the matrix element and parton shower calculations [26]. All stable particles with lifetime $c\tau > 1$ cm after showering and hadronization are clustered into jets with the FASTJET package [27] using the anti-kT algorithm with a distance parameter of 0.4.

Various simulated samples are generated for this study; a SM sample ($C_G = 0$), a SM plus O_G sample including the SM-O_G interference, and a pure O_G sample without including SM-O_G interference. The interference effects were evaluated by comparing the prediction of the SM plus O_G (with O_G-SM interference) sample to the sum of pure SM and pure O_G samples for distributions of various kinematic observable including χ_{dijet}. The interference effects are found to be negligible compared to the statistical and theoretical uncertainties for $C_G/\Lambda^2 = 1$ TeV^{-2} [7,8]. This is expected because of the different helicity structure between the SM and O_G interactions, as mentioned earlier. Also, the interference effects vary linearly as a function of C_G and become smaller for lower values of C_G. Therefore, based on the current limits on the C_G coupling, the interference effects are ignored in this analysis and the pure O_G sample is considered as the signal. The differential jet rate (DJR) distributions are used to check the validity of the merging procedure in the presence of the O_G operator. The O_G operator does not lead to soft and colinear divergences [28] and the DJR distributions are found to be smooth.

3. Data and SM prediction

In order to evaluate the power of the dijet angular distributions for probing the C_G coupling, we focus on a recent analysis [17] performed by the CMS Collaboration at $\sqrt{s} = 13$ TeV and with an integrated luminosity of 35.9 fb^{-1}. In this analysis, normalized dijet angular distributions, denoted as $(1/\sigma_{dijet})(d\sigma_{dijet}/d\chi_{dijet})$, are measured over a wide range of di-jet invariant masses and the results are used to probe parameter spaces of various new physics models. We use the public information provided by the CMS Collaboration in the HEPDATA database. In particular, we employ the data and SM prediction with the corresponding uncertainties.

Events are required to have at least two reconstructed jets with $p_T > 200$ GeV and $|\eta| < 2.5$, where η is the jet pseudo-rapidity. The two jets with the highest p_T are used to make the dijet system and are required to have $|y_{boost}| < 1.11$, where $y_{boost} = (y_1 + y_2)/2$. Events are further categorized in the following bins of the dijet invariant mass (m_{jj}); [2.4,3.0), [3.0,3.6), [3.6,4.2), [4.2,4.8), [4.8,5.4), [5.4,6.0), and >6.0 TeV. The χ_{dijet} distributions are normalized to unity in each mass range and are then unfolded to the particle level. The contribution of the SM multijet production is predicted at next-to-leading order QCD using NLOJET++4.1.3 [29] including electroweak corrections [30].

Various experimental and theoretical uncertainties are considered in this measurement [17]. In general, the normalized differential cross sections in χ_{dijet} are relatively insensitive to many systematic effects. The importance of the uncertainty sources varies

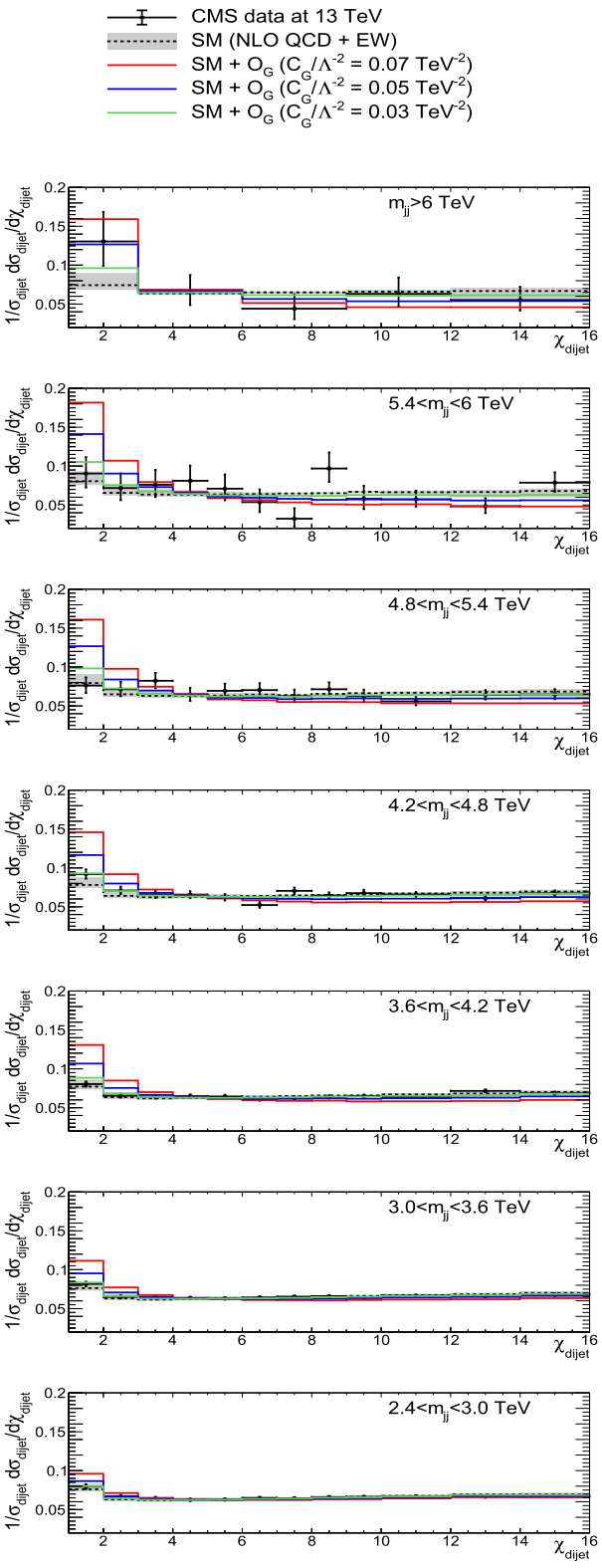

Fig. 1. Normalized distributions of the dijet angular variable, χ_{dijet}, in different regions of the dijet invariant mass m_{jj}. The data (points) and the total theoretical and experimental uncertainties are measured by the CMS Collaboration [17] and are displayed as shaded bands around the SM prediction. The SM plus O_G expectation is shown for three arbitrary values of the C_G coupling.

from the low to high dijet mass bins. In the lowest mass bin, the theoretical uncertainties are dominant, while in the highest dijet mass the dominant source is the statistical uncertainty. The quadratic sum of all systematic uncertainties for all bins of χ_{dijet} is also provided in HEPDATA and is used in this analysis.

4. Results

In Fig. 1, the normalized χ_{dijet} distributions of the unfolded data are compared to the SM predictions and to the predictions of the SM plus O_G for various C_G values in all mass bins. The data points, SM QCD predictions, and associated uncertainties are imported directly from HEPDATA [17]. We have used our simulated sample to find the normalized χ_{dijet} distributions for the signal. Thus, the template of dijet angular distributions for the SM includes NLO QCD plus EW corrections while the contribution of the signal is predicted at LO. For these plots, the ratio of the O_G contribution to that of the SM is taken directly from the ratio of the predicted cross sections in the leading-order QCD and signal MC samples after corrections for the fiducial acceptance. Cross section ratios are provided for $C_G/\Lambda^2 = 1$ in Table I. Here, the area of the sum of the O_G and SM contributions has been normalized to unity for each value of C_G/Λ^2 so that the differences in the shapes of the distributions are easily compared. As can be seen in the figure, the contribution of the O_G operator peaks at small values of χ_{dijet}, contrary to the expectation from SM QCD.

In order to set constraints on the C_G coupling, we used the modified frequentist CLs method [31,32]. We performed a binned likelihood fit that determined the best fit ratio of O_G to SM MC distributions that described the data. The systematic uncertainties in the SM prediction are imported bin by bin from the HEPDATA. The systematic uncertainties in each bin of the χ_{dijet} distribution are correlated to the same χ_{dijet} bin in other dijet mass regions using the covariance matrices provided by the CMS Collaboration in HEPDATA. We have considered three sources of uncertainty on the signal prediction: renormalization and factorization scale uncertainty, PDF uncertainties and the uncertainty due to a finite number of simulated events. The effect of the renormalization and factorization scale uncertainty is estimated by varying the scales used during the generation of the signal sample independently by a factor 0.5 to 2. The envelope of the variations in each bin is taken as the renormalization and factorization scale uncertainty. The PDF uncertainty on the signal prediction is calculated using the replicas of the NNPDF 3.0 set. Correlations of these uncertainties across χ_{dijet} and dijet mass bins are included. The PDF uncertainty in the first bin of the normalized χ_{dijet} distribution increases significantly from 0.4% for the lowest mass bin to 35% for the highest mass bin. The Q-scale uncertainty varies between 0.2% to 1.7% for the lowest χ_{dijet} bin in different mass bins. In addition, the Q-scale and PDF uncertainties on the SM QCD background that are reported by the CMS Collaboration at NLO are inserted to our statistical analysis directly from the HEPDATA tables [17]. To convert the best-fit ratios of the normalized dijet angular distributions into limits on C_G/Λ^2, we use the ratios of the SM cross section to the O_G cross section given in Table I, which varies as a function of the dijet mass. Limits on the fractional contribution of the O_G shape to the overall distribution are transformed using these ratios to limits on the cross section for the O_G process, and hence to a value of C_G/Λ^2.

The observed (expected) 95% CL limit on the C_G Wilson coefficient obtained from the combination of all mass bins is 0.034 (0.018) TeV^{-2}. Based on the expected limits, the most sensitive mass bins are [3.6,4.2), [3.0,3.6) and [4.2,4.8) TeV with the expected limit $C_G/\Lambda^2 < 0.021$, 0.022, and 0.025 TeV^{-2}, respectively. The weakest expected limit is found from the highest mass bin (>6.0), $C_G/\Lambda^2 < 0.062$ TeV^{-2} because of the large statistical errors. The obtained limit does not depend strongly on the very high mass bins where the applicability of the SMEFT might be less valid because of the high energy scales involved. This dependence was explicitly checked by removing all di-jet events with

Table I
The cross section ratio of multijet production with one O_G vertex to the SM at leading order for $C_G^2/\Lambda^4 = 1/\text{TeV}^4$ in the fiducial region for the considered mass bins.

Mass bin (TeV)	>2.4.0	[2.4,4.8]	[2.4,3.0]	[3.0,3.6]	[3.6,4.2]	[4.2,4.8]	[4.8,5.4]	[5.4,6.0]	>6.0
σ_{O_G}/σ_{SM}	17.2	16.9	13.2	24.2	38.6	53.2	67.7	89.7	112.4

Table II
Observed and expected exclusion limits on the C_G/Λ^2 at 95% CL. The 68% and 95% ranges of expectation for the expected limit are given as well.

Mass bins	Observed (TeV^{-2})	Expected (TeV^{-2})	68% range (TeV^{-2})	95% range (TeV^{-2})
[2.4,3.0]	0.034	0.026	[0.022,0.031]	[0.019,0.035]
[3.0,3.6]	0.034	0.022	[0.019,0.026]	[0.016,0.030]
[3.6,4.2]	0.027	0.021	[0.018,0.025]	[0.015,0.029]
[4.2,4.8]	0.037	0.025	[0.021,0.029]	[0.018,0.034]
[4.8,5.4]	0.035	0.032	[0.026,0.037]	[0.023,0.044]
[5.4,6.0]	0.041	0.038	[0.032,0.046]	[0.027,0.054]
>6.0	0.077	0.062	[0.043,0.066]	[0.037,0.082]
First 4 bins combined	0.032	0.019	[0.016,0.023]	[0.014,0.031]
All bins combined	0.034	0.018	[0.015,0.021]	[0.013,0.027]

center-of-mass energy greater than 5.4 TeV from the SM and signal samples, and recomputing the limits. No change was observed. We also found the expected and observed limit combining the four low mass bins $C_G/\Lambda^2 < 0.019$ TeV^{-2} and $C_G/\Lambda^2 < 0.032$ TeV^{-2}, respectively. The observed and expected exclusion limits at 95% CL obtained from different mass bins are listed in Table II. The observed limits are weaker than the expected limits because of an overall excess of events in the first χ_{dijet} bin at all mass scales. This effect was also seen in the published CMS analysis.

5. Conclusions and prospects

In this paper, we have presented a detailed analysis of the dimension-6 triple gluon operator O_G, improving the constraints on its potential influence using an analysis sensitive to the helicity structure of the operator. We note that, to lowest order, there is no interference of the effects of O_G with standard QCD amplitudes in $2 \to 2$ processes. This implies that the effects of O_G should be purely additive, making the analysis easy to interpret. We have shown that the dijet angular variable χ_{dijet} has good sensitivity to anomalous large values of C_G, the Wilson coefficient of O_G. Using public data from the CMS experiment, we have set a limit of $C_G/\Lambda^2 < 0.034$ TeV^{-2} at 95% confidence level, the most stringent limit to date on C_G. Even with the improved sensitivity of this result, the analysis suffers from constraints related to the use of public data. The use of relative cross sections for limit-setting cancels some systematic errors but does not give full sensitivity to variations in production cross sections. In addition, the original CMS simulated samples are not available, so some systematic errors could be reduced by careful studies. We believe, however, that the LHC experiments could produce significantly improved limits on C_G using this technique and the full Run 2 dataset. In principle, a characterization of C_G should be included in SMEFT studies so as to independently constrain the value of C_G and its effects on the other dimension-6 operators that can be observed in Higgs boson and top quark events.

Declaration of competing interest

The authors declare that they have no known competing financial interests or personal relationships that could have appeared to influence the work reported in this paper.

Acknowledgement

We would like to thank B. Clerbaux, H. Bakhshian and A. Jafari for valuable discussions.

References

[1] B. Grzadkowski, et al., Dimension-six terms in the standard model Lagrangian, J. High Energy Phys. 10 (2010) 085, arXiv:1008.4884.
[2] W. Buchmuller, D. Wyler, Effective Lagrangian analysis of new interactions and flavor conservation, Nucl. Phys. B 268 (1986) 621–653.
[3] A. Buckley, et al., Constraining top quark effective theory in the LHC Run II era, J. High Energy Phys. 04 (2016) 015, arXiv:1512.03360.
[4] J. Ellis, et al., Updated global SMEFT fit to Higgs, diboson and electroweak data, J. High Energy Phys. 06 (2018) 146, arXiv:1803.03252.
[5] N.P. Hartland, et al., A Monte Carlo global analysis of the standard model effective field theory: the top quark sector, J. High Energy Phys. 04 (2019) 100, arXiv:1901.05965.
[6] D. Ghosh, M. Wiebusch, Dimension-six triple gluon operator in higgs+jet observables, Phys. Rev. D 91 (2015) 031701, arXiv:1411.2029.
[7] V. Hirschi, et al., Constraining anomalous gluon self-interactions at the LHC: a reappraisal, J. High Energy Phys. 07 (2018) 093, arXiv:1806.04696.
[8] F. Krauss, et al., LHC multijet events as a probe for anomalous dimension-six gluon interactions, Phys. Rev. D 95 (2017) 035024, arXiv:1611.00767.
[9] E.H. Simmons, Dimension-six gluon operators as probes of new physics, Phys. Lett. B 226 (1989) 132–136.
[10] E.H. Simmons, Higher dimension gluon operators and hadronic scattering, Phys. Lett. B 246 (1990) 471–476.
[11] L.J. Dixon, Y. Shadmi, Testing gluon selfinteractions in three jet events at hadron colliders, Nucl. Phys. B 423 (1994) 3–32, arXiv:hep-ph/9312363.
[12] P.L. Cho, et al., Searching for G3 in $t\bar{t}$ production, Phys. Rev. D 51 (1995) 2360–2370, arXiv:hep-ph/9408206.
[13] CMS Collaboration, Search for new physics in top quark production in dilepton final states in proton-proton collisions at $\sqrt{s}$ = 13 TeV, Eur. Phys. J. C 79 (2019) 886, arXiv:1903.11144.
[14] E. Eichten, et al., Supercollider physics, Rev. Mod. Phys. 56 (Oct. 1984) 579–707.
[15] E.J. Eichten, et al., New tests for quark and lepton substructure, Phys. Rev. Lett. 50 (Mar 1983) 811–814.
[16] H. Terazawa, Subquark model of leptons and quarks, Phys. Rev. D 22 (Jul. 1980) 184–199.
[17] CMS Collaboration, A.M. Sirunyan, et al., Search for new physics in dijet angular distributions using proton–proton collisions at $\sqrt{s}$ = 13 TeV and constraints on dark matter and other models, Eur. Phys. J. C 78 (2018) 789, arXiv:1803.08030.
[18] ATLAS Collaboration, Search for new phenomena in dijet events using 37 fb^{-1} of pp collision data collected at $\sqrt{s}$ =13 TeV with the ATLAS detector, Phys. Rev. D 96 (2017) 052004, arXiv:1703.09127.
[19] S. Alte, et al., Consistent searches for SMEFT effects in non-resonant dijet events, J. High Energy Phys. 01 (2018) 094, arXiv:1711.07484.
[20] A. Alloul, et al., FeynRules 2.0 - a complete toolbox for tree-level phenomenology, Comput. Phys. Commun. 185 (2014) 2250–2300, arXiv:1310.1921.
[21] C. Degrande, et al., UFO - the universal FeynRules output, Comput. Phys. Commun. 183 (2012) 1201–1214, arXiv:1108.2040.
[22] J. Alwall, et al., The automated computation of tree-level and next-to-leading order differential cross sections, and their matching to parton shower simulations, J. High Energy Phys. 07 (2014) 079, arXiv:1405.0301.
[23] NNPDF Collaboration, Parton distributions for the LHC Run II, J. High Energy Phys. 04 (2015) 040, arXiv:1410.8849.
[24] T. Sjostrand, et al., A brief introduction to PYTHIA 8.1, Comput. Phys. Commun. 178 (2008) 852–867, arXiv:0710.3820.
[25] CMS Collaboration, Event generator tunes obtained from underlying event and multiparton scattering measurements, Eur. Phys. J. C 76 (2016) 155, arXiv:1512.00815.

[26] M.L. Mangano, et al., ALPGEN, a generator for hard multiparton processes in hadronic collisions, J. High Energy Phys. 07 (2003) 001, arXiv:hep-ph/0206293.
[27] M. Cacciari, et al., FastJet user manual, Eur. Phys. J. C 72 (2012) 1896, arXiv:1111.6097.
[28] C. Englert, et al., Effective field theory in the top sector: do multijets help?, Phys. Rev. D 99 (2019) 035019, arXiv:1809.09744.
[29] T. Kluge, et al., FastNLO: fast pQCD calculations for PDF fits, in: Deep Inelastic Scattering. Proceedings, 14th International Workshop, DIS 2006, Tsukuba, Japan, April 20-24, 2006, 2006, pp. 483–486, arXiv:hep-ph/0609285.
[30] S. Dittmaier, et al., Weak radiative corrections to dijet production at hadron colliders, J. High Energy Phys. 11 (2012) 095, arXiv:1210.0438.
[31] T. Junk, Confidence level computation for combining searches with small statistics, Nucl. Instrum. Methods A 434 (1999) 435–443, arXiv:hep-ex/9902006.
[32] A.L. Read, Presentation of search results: the CLs technique, J. Phys. G, Nucl. Part. Phys. 28 (2002) 2693–2704.